Suppression of Microtubule Dynamics by Binding of Cemadotin to Tubulin: Possible Mechanism for Its Antitumor Action†

Mary Ann Jordan,*,‡ Deborah Walker,‡ Monika de Arruda,§,|| Teresa Barlozzari,§ and Dulal Panda‡

Department of Molecular, Cellular, and Developmental Biology, University of California, Santa Barbara, California 93106, and BASF Bioresearch Corporation, Worcester, Massachusetts 01605

Received July 20, 1998; Revised Manuscript Received September 21, 1998

ABSTRACT: Cemadotin (LU103793) (NSC D-669356) is a water-soluble synthetic analogue of dolastatin 15 that inhibits cell proliferation in vitro and the growth of human tumor xenografts. Cemadotin is in phase II clinical trials as a promising cancer chemotherapeutic agent. The drug blocks cells at mitosis. Its primary mode of action has been unclear but is believed to involve an action on microtubules. We have found that cemadotin binds to tubulin and strongly suppresses microtubule dynamics. Scatchard analysis of cemadotin binding to tubulin indicated that there are two affinity classes of cemadotin-binding sites with K_d values of 19.4 μM and 136 μM. Cemadotin did not inhibit the binding of vinblastine to tubulin, and, conversely, vinblastine did not inhibit the binding of cemadotin to tubulin. By quantitative video microscopy of individual microtubules, we found that cemadotin strongly suppressed dynamic instability of microtubules assembled to steady state using bovine brain tubulin devoid of microtubule-associated proteins. It reduced the rate and extent of growing and shortening, increased the rescue frequency, and increased the percentage of time the microtubules spent in an attenuated or paused state, neither growing nor shortening detectably. At the lowest effective cemadotin concentrations, dynamics were suppressed in the absence of significant microtubule depolymerization. The results suggest that cemadotin exerts its antitumor activity by suppressing spindle microtubule dynamics through a distinct molecular mechanism by binding at a novel site in tubulin.

Cemadotin (LU103793) (NSC D-669356) (Figure 1) is a novel cytotoxic water-soluble pentapeptide analogue of dolastatin 15. The dolastatin peptides were originally isolated from the shell-less mollusc *Dolabella auricularia*. Extracts of this marine animal were employed in ancient Roman times to poison the emperor Claudius and his stepson [reviewed by Luduena et al. (*1*)]. More recently they were found to strongly inhibit proliferation of the murine P388 lymphocytic leukemia cells (*2*). Among the 15 novel cytotoxic peptides (dolastatins 1−15) that were ultimately isolated from extracts, two of the natural compounds potently inhibit cell proliferation in a wide variety of leukemia cell lines (*3*), block mitosis at G2/M phase in lymphoma cell lines (*4*), and are undergoing clinical trials (*5*).

However, the synthesis of naturally occurring dolastatins is complex and yields low amounts of product, and their poor aqueous solubility may limit clinical application. To overcome these problems, numerous analogues of dolastatin 15 were synthesized and tested in human tumor xenograft models. These efforts yielded the pentapeptide cemadotin (LU103793), which potently inhibits proliferation of a number of human carcinoma cell lines including mammary (MDA-MB435), colon (HT-29), and cervical (HeLa S3) carcinoma cell lines (with IC_{50} values of 0.1 nM, 0.6 nM, and 0.7 nM, respectively) (*6*). Cemadotin is currently in phase II clinical trials as a promising cancer chemotherapeutic agent for metastatic melanoma and other solid tumors. Inhibition of cell proliferation by cemadotin occurs at metaphase of mitosis and is not associated with inhibition of DNA synthesis. The drug is hypothesized to work by an interaction with tubulin and /or microtubules. It inhibits microtubule polymerization and depolymerizes preformed microtubules in vitro. At low concentrations it disrupts cellular spindle microtubule organization in a manner resembling the disruption induced by several other drugs that act on microtubules, including vinblastine, colchicine, and paclitaxel (*7*−*9*). However, like the parent compound dolastatin 15, the binding of cemadotin to tubulin has not been detected and the drug does not significantly inhibit the binding of other tubulin ligands such as vinblastine or colchicine (*10*, *6*). Thus the antitumor mechanism of cemadotin and the nature of its interaction with tubulin and microtubules remain open questions.

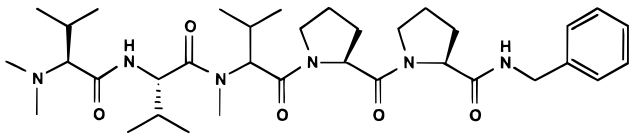

LU103793

FIGURE 1: Structure of cemadotin (LU103793).

Microtubules are involved in a variety of cell processes including intracellular transport, shape determination, and mitosis. They are intrinsically dynamic, long tube-shaped

† Supported in part by NIH CA57291 (M.A.J.).

* To whom correspondence should be addressed: phone 805-893-5317; FAX 805-893-4724; email jordan@lifesci.lscf.ucsb.edu.

‡ University of California.

§ BASF Bioresearch Corp.

|| Present address: Third Wave Technology, Inc., Madison, WI.

10.1021/bi9817414 CCC: $15.00
Published on Web 11/20/1998

polymers composed of $\alpha\beta$ tubulin heterodimers (*11*). Microtubule ends switch between growing and shortening states, a behavior termed dynamic instability, apparently due to a stochastic gain and loss at the microtubule ends of a stabilizing GTP or GDP·Pi cap (*12*−*16*). Recent evidence indicates that the dynamics of microtubules, not just their presence, are critically involved in microtubule function (*17*−*19*). For example, microtubule dynamics are essential for chromosome movement during mitosis, which involves dynamic interactions between the kinetochores of the chromosomes and the spindle microtubules.

Microtubules and their dynamics are the principal targets of several antimitotic chemotherapeutic compounds (*20*). For example, vinblastine and colchicine are potent inhibitors of microtubule polymerization that inhibit cell proliferation at prometaphase of mitosis (*19*, *21*, *22*). Taxol, which increases microtubule polymerization, similarly inhibits mitosis at metaphase (*9*). While all three drugs produce profound effects on the microtubule polymer mass at relatively high drug concentrations, we have found that, at low concentrations, they appear to inhibit proliferation of HeLa cells at mitosis by suppressing microtubule dynamics. Mitotic block ultimately results in cell death (*23*). These results have indicated that the most potent chemotherapeutic mechanism by which antimitotic drugs act to inhibit proliferation and induce death of tumor cells is by suppression of spindle microtubule dynamics rather than by depolymerization or excessive polymerization of spindle microtubules (*7*, *9*, *19*, *20*, *22*, *24*, *25*).

In the present study, we sought to elucidate the antitumor mechanism of cemadotin by examining its binding to tubulin and its interactions with microtubules. By fluorescence spectroscopy and binding of radiolabeled drug, we found that cemadotin binds with high affinity to an apparently unique site on tubulin and suppresses the dynamics of individual microtubules by a distinct molecular mechanism.

EXPERIMENTAL PROCEDURES

Purification of Tubulin. Bovine brain microtubule protein was isolated without glycerol by three cycles of polymerization and depolymerization. Tubulin was purified from the microtubule protein by phosphocellulose chromatography (*26*). The tubulin solution was rapidly frozen as drops in liquid nitrogen and stored at −70 °C until used. Protein concentration was determined by the method of Bradford (*27*) with bovine serum albumin as the standard.

Microtubule Polymerization and Determination of Steady-State Microtubule Polymer Mass. Tubulin pellets were thawed and centrifuged at 4 °C to remove any aggregated or denatured tubulin. Tubulin (18 μM) was mixed with *Strongylocentrotus purpuratus* flagellar axonemal seeds (*26*) in 86 mM Pipes,[1] 36 mM Mes, 1.4 mM $MgCl_2$, and 1 mM EGTA, pH 6.8 (assembly buffer), containing 1 mM GTP and incubated (37 °C) in the absence or presence of a range of concentrations of cemadotin for 1 h to polymerize the microtubules. The microtubules were collected by centrifugation (150000*g*, 1 h, 37 °C) and the microtubule pellets were solubilized in distilled water for determination of protein concentration.

Determination of Microtubule Dynamic Instability. Tubulin (12 μM) was mixed with axoneme seeds and polymerized in assembly buffer containing 1 mM GTP in the presence or absence of cemadotin. The seed concentration was adjusted to achieve 3−6 seeds/microscope field. After 35 min of incubation, samples of microtubule suspensions (2.5 μL) were prepared for differential interference contrast videomicroscopy and the dynamics of individual microtubules were recorded at 37 °C as previously described (*26*). The microtubules were observed for a maximum of 45 min after they had reached steady state. Under the experimental conditions used, microtubule growth occurred predominantly at the plus ends of the seeds as determined by the growth rates, the number of microtubules that grew, and the relative lengths of the microtubules at the opposite ends of the seeds (*14*, *26*, *28*). Microtubule length changes were analyzed as described previously (*28*). We considered the microtubule to be in a growing phase if the microtubule increased in length by >0.2 μm at a rate $>$ 0.15 μm/min and in a shortening phase if the microtubule shortened in length by $>$ 0.2 μm at a rate $>$ 0.3 μm/min. Length changes equal to or less than 0.2 μm over the duration of 6 data points were considered as attenuation or pause phases. We used the same tubulin preparation for all experiments. An average of 13 microtubules was measured for each experimental condition.

The catastrophe frequency [a catastrophe is a transition from the growing or attenuated state to shortening (*14*)] was calculated by dividing the number of catastrophes by the sum of the total time spent in the growing plus attenuated states for all microtubules for a particular condition. The rescue frequency [a rescue is a transition from shortening to growing or attenuation, excluding new growth from a seed (*14*)] was calculated by dividing the total number of rescue events by the total time spent shortening for all microtubules for a particular condition. The average length the microtubules grew per growing event was determined by dividing the summed growing lengths for all microtubules for a particular condition by the total number of growing events. The average length shortened per shortening event was determined analogously.

Fluorescence Measurements. The interaction of cemadotin with tubulin (2 μM) was monitored by using the fluorescence of tubulin−bis-ANS or of tubulin−ANS (*29*) measured with a Perkin-Elmer LS50B spectrofluorometer equipped with a constant-temperature water circulating bath (34 °C). Spectra were taken by multiple scans, and buffer blank values were subtracted from all measurements. The intrinsic tubulin fluorescence change induced upon the binding of cemadotin to tubulin was measured with 295 nm as the excitation wavelength, and emission at 337 nm was used for calculations. The excitation and emission band-pass were 10 nm.

Cemadotin Binding to Tubulin. Cemadotin, 2−200 μM, spiked with a trace of [^{14}C]cemadotin (specific activity 892 MBq/mmol)(synthesized by BASF Pharma, Ludwigshafen/Rhein, Germany) was mixed with tubulin (5 μM) in assembly buffer and incubated (4 °C, 40 min). Bound drug was determined by use of an MPS micropartition device with YMT membrane (Amicon, Beverly, MA) centrifuged at 4500 rpm for 90 s (Sorvall, SS35 rotor, 4 °C) (*30*). The MPS micropartition device was preincubated with 1% aqueous nonfat dried milk overnight (25 °C) to reduce adhesion of

[1] Abbreviations: ANS, 1-anilino-8-naphthalenesulphonate; bis-ANS, bis-8-anilino-1-naphthalenesulfonic acid; Pipes, 1,4-piperazinediethanesulfonic acid; Mes, 2-morpholinoethanesulfonic acid.

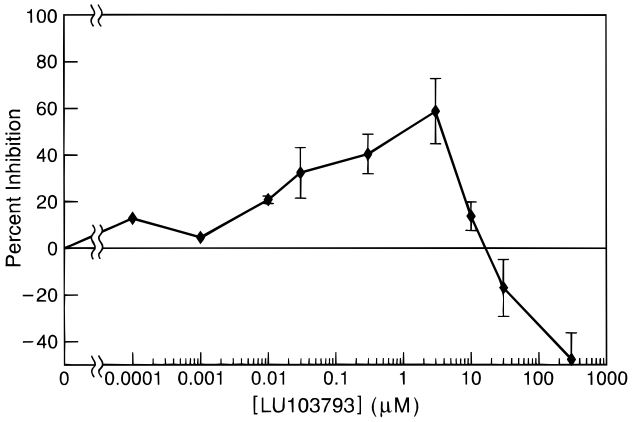

FIGURE 2: Effects of cemadotin on steady-state microtubule polymer mass. Tubulin (18 μM) was mixed with *S. purpuratus* flagellar seeds in assembly buffer containing 1 mM GTP and incubated at 37 °C in the absence or presence of different concentrations of cemadotin for 35 min to polymerize the microtubules to steady state. The microtubules or tubulin aggregates were pelleted by centrifugation at 150000*g* for 1 h and the pellets were solubilized at 0 °C for protein determination. Error bars = SEM.

cemadotin to the apparatus. The concentration of unbound cemadotin was determined by measuring the radioactivity in the centrifugate, and bound ligand was determined by subtracting unbound ligand from total ligand. Nonspecific adhesion was determined following centrifugation in the absence of tubulin. The association constant for the tubulin−cemadotin interaction was calculated according to the method of Scatchard (*31*).

Binding of [^{14}C]cemadotin to tubulin in the presence of vinblastine was determined by column centrifugation (*32*). Tubulin (6 μM) and cemadotin (10 μM) containing [^{14}C]-cemadotin were incubated with or without vinblastine (0−50 μM) at 0 °C for 30 min. Tubulin-bound cemadotin was separated from unbound cemadotin by centrifugation with 1-mL columns of Bio-Gel P6 (Bio-Rad). Radioactivity and proteins in the eluates were determined. Background radioactivity measured in the absence of tubulin was subtracted from the experimental values.

RESULTS

Inhibition of Microtubule Polymerization by Cemadotin. The ability of cemadotin to inhibit axoneme-seeded microtubule polymerization of bovine brain tubulin was determined by measuring polymer mass with a sedimentation assay (Experimental Procedures). As shown in Figure 2, cemadotin inhibited polymerization in a concentration-dependent manner; 50% inhibition occurred at 1 μM compound. The lowest concentration of cemadotin that significantly reduced the microtubule polymer mass (by 21%) was 10 nM (Figure 1). At concentrations of cemadotin greater than 3 μM, the mass of polymerized tubulin increased, consistent with previous observations of the formation of tubulin aggregates in the form of ring structures at high concentrations of cemadotin (>50 μM) (*6*).

Dynamic Instability of Control Microtubules at Steady State. Microtubules were polymerized from bovine brain tubulin with axonemal fragments as seeds (see Experimental Procedures). Microtubule growth occurred predominantly at the plus ends of the seeds. Several "life history" traces

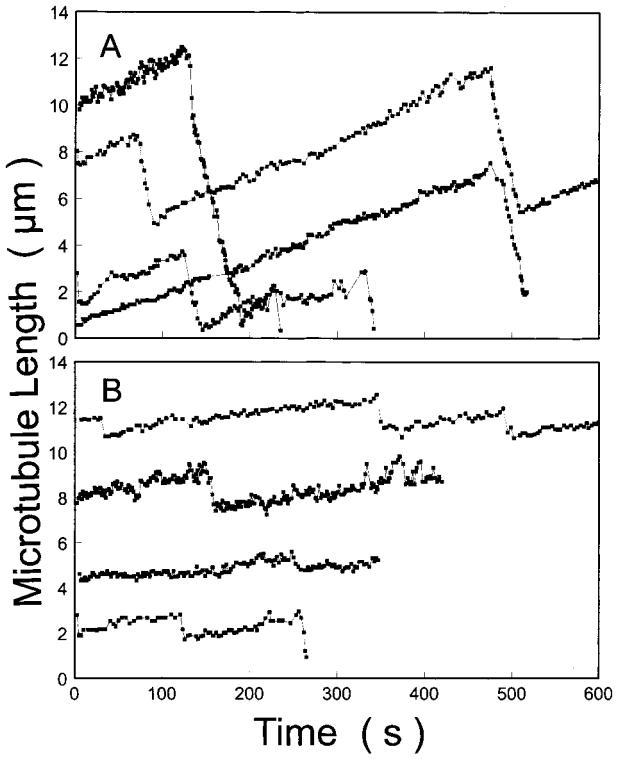

FIGURE 3: Growing and shortening length changes of microtubules at their plus ends at steady state in the absence (A) and presence of 0.1 μM (B) cemadotin. The lengths of individual microtubules were measured from real-time videotape recordings as described under Experimental Procedures.

showing typical length changes at the plus ends of control microtubules in the absence of drug are shown in Figure 3A. Life history traces were used to determine the parameters of dynamic instability (Table 1). As previously documented, control microtubules alternated between phases of slow growing (26.1 ± 2.9 dimers/s) and rapid shortening (284 ± 31 dimers/s) and also spent a small fraction of time (9%) in an attenuated or pause state, neither growing nor shortening detectably.

Cemadotin Preferentially Suppressed the Rate and Extent of Growing Excursions. As shown in Figure 3B, addition of cemadotin at concentrations as low as 100 nM suppressed microtubule dynamics. The rates and extents of growing and shortening events were reduced and the percentage of time that the microtubules spent in the attenuated or pause state was increased. As shown in Figure 4, cemadotin more strongly suppressed the growing rates than the shortening rates, and suppression was dependent upon the drug concentration. For example, 100 nM cemadotin reduced the mean growing rate by 41% (to 15.3 ± 2.5 dimers/s). At the highest concentration studied (1 μM), cemadotin reduced the mean growing rate by approximately 63% to 9.7 ± 1.3 dimers/s. The average length the microtubules grow per growing event is considered to be important in the "search and capture" mechanism of attachment of dynamic microtubules to prometaphase chromosomes. The length grown per growing event was strongly decreased by cemadotin (Table 1). For example, at 100 nM cemadotin the mean growing length was reduced ~46% from 2.2 μm per growing event to 1.2 μm per event. Thus, microtubules grew more slowly and grew less extensively in the presence of cemadotin than in its absence.

Table 1: Effects of Cemadotin on the Dynamic Instability Parameters of Microtubule Plus Ends at Steady State

	cemadotin (nM)					
	0	0.1	1.0	10	100	1000
			Rate (dimer s^{-1})			
growing	26.1 ± 2.9[a]	26.9 ± 1.8	19.7 ± 2.2	19.7 ± 2.2	15.3 ± 2.5	9.7 ±1.3
shortening	284 ± 31	313 ± 30	309 ± 32	261 ± 42	214 ± 45	147 ± 40
			Mean Length Grown or Shortened per Event (μm)			
growing	2.2	2.0	1.9	1.0	1.2	0.6
shortening	5.5	5.9	4.9	4.0	3.3	3.0
			Phase Duration (s)			
growing	141 ± 21	126 ± 16	162 ± 24	88 ± 12	131 ± 18	107 ± 11
shortening	33 ± 3	32 ± 3	27 ± 4	26 ± 4	26 ± 1	35 ± 6
pause	58 ± 14	74 ± 6	62 ± 15	55 ± 13	82 ± 8	90 ± 14
			Percent of Total Time			
growing	76	71	81	63	77	59
shortening	15	17	10	17	10	11
pause	9	11	8	21	13	30
			Frequency (s^{-1})			
rescue	0.010	0.015	0.017	0.023	0.033	0.030
catastrophe	0.0054	0.0067	0.0040	0.0079	0.0041	0.0036
			Frequency (μm^{-1})			
rescue	0.071	0.088	0.105	0.209	0.297	0.496
catastrophe	0.56	0.63	0.43	1.11	0.74	1.34
			Dynamicity (dimers/s)			
	62.5	72.9	48.4	56.9	32.7	21.9

[a] Standard error of mean.

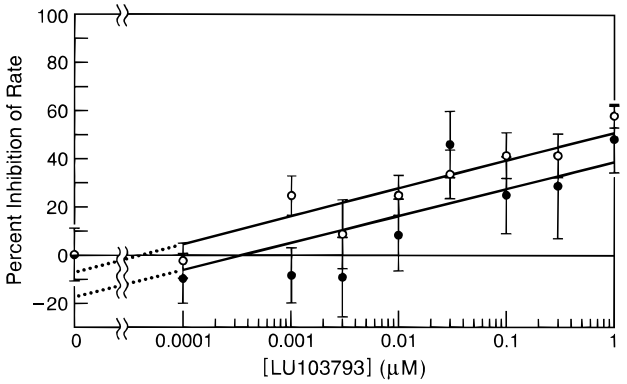

FIGURE 4: Suppression of the rates of growing (○) or shortening (●) at microtubule ends by cemadotin. The rates of individual microtubule growing and shortening events were measured from real-time videotape recordings as described in Experimental Procedures. Error bars = SEM.

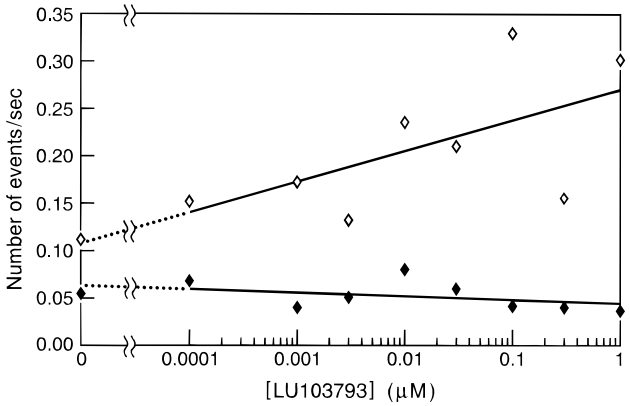

FIGURE 5: Effects of cemadotin on the frequency of rescue or catastrophe calculated on the basis of time. Number of rescues per second in the shortening phase (◊) and number of catastrophes per second in the phases of growing and attenuation (♦) as a function of cemadotin concentration (see Experimental Procedures).

Cemadotin also suppressed the rate and extent of shortening, but its effect on shortening was less than its effect on growing (Table 1; Figure 4). For example, at 100 nM cemadotin the shortening rate was reduced 25% (from 284 ± 31 dimers/s in controls to 214 ± 45 dimers/s) and the mean length shortened during a shortening event was reduced by 40% (from 5.5 to 3.3μm per shortening event).

Cemadotin inhibited dynamic instability to approximately the same degree as it reduced the polymer mass (inhibition at 100 nM drug: growing rate, 41%; shortening rate, 25%; growing length, 46%; shortening length, 40%; as compared with 35% reduction in polymer mass) (Table 1). Thus, the sensitivity of dynamic instability to cemadotin was similar to the sensitivity of bulk polymerization.

Cemadotin Markedly Increased the Rescue Frequency but Had Little Effect on the Catastrophe Frequency. The frequencies of transition among the growing, shortening, and pause states are considered to be important in the regulation of microtubule dynamics and function in cells (*33*, *34*). Transition frequencies can be calculated on the basis of the time spent growing or shortening (Figure 5, Table 1) as well as on the basis of microtubule length grown or shortened (Table 1) (*25*, *35*). Cemadotin markedly increased the frequency of rescue from episodes of shortening. For example, 100 nM cemadotin increased the time-based rescue frequency 3-fold (from 0.010 to 0.033 s^{-1}) and the length-based rescue frequency 4-fold (from 0.07 to 0.30 μm^{-1}). In contrast, the drug had little or no effect on the time-based catastrophe frequency and only slightly increased the length-based catastrophe frequency (~1.4-fold). The net result was that microtubules transitioned to rapid shortening as often in the presence of cemadotin as in controls, but the lengths shortened were very short, resulting in marked kinetic stabilization of microtubule dynamics.

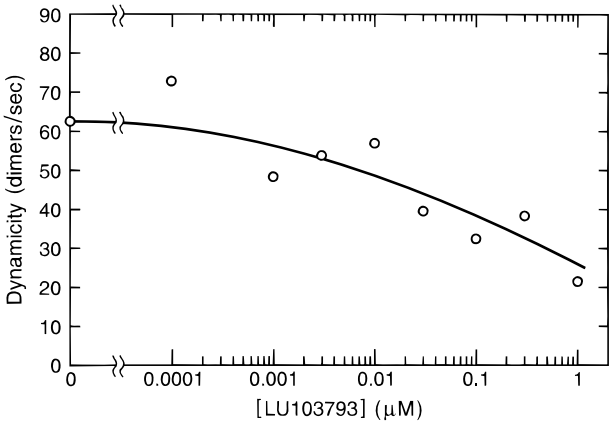

FIGURE 6: Suppression of dynamicity by cemadotin. Dynamicity, a measure of overall dynamics, was calculated from all detectable growing and shortening length changes including the time microtubules spent in the attenuated state (see Experimental Procedures).

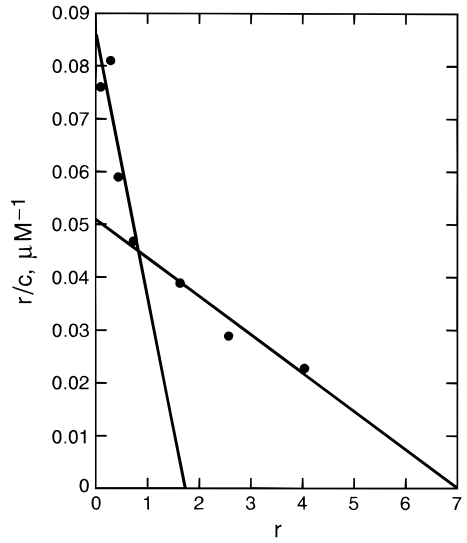

FIGURE 7: Scatchard plot of the binding of cemadotin to tubulin. Tubulin (5 μM) was incubated with different concentrations of cemadotin (2−200 μM) containing a trace of [^{14}C]cemadotin at 4 °C for 15 min. Bound drug was determined by use of an MPS micropartition device with YMT membrane (see Experimental Procedures). r = [bound cemadotin]/[tubulin]; c = [unbound cemadotin], in micromolar.

Dynamicity is a parameter that reflects the overall dynamics of the microtubules [the total detectable tubulin dimer addition and loss at a microtubule end including the time spent in the attenuated state (*22*, *26*)]. As shown in Figure 6, dynamicity was strongly suppressed by cemadotin. At 100 nM drug, for example, dynamicity was suppressed by 48%.

Cemadotin Binds to Tubulin. Using an equilibrium technique with a micropartitioning system, we were able to detect and examine the binding of [^{14}C]cemadotin to tubulin over a wide range of drug concentrations at 0 °C (see Experimental Procedures). Scatchard analysis of the data was biphasic (Figure 7), indicating two affinity classes of binding sites. The slopes of the curves yielded a K_d of 19.4 μM and a stoichiometry of 0.91 for the high-affinity site and a K_d of 136 μM for the low-affinity binding to multiple sites. The weak affinity of cemadotin for multiple sites in tubulin suggests that binding to these sites may be nonspecific. Alternatively, these low-affinity sites may be generated by the aggregation of tubulin dimers in the presence of high concentrations of cemadotin.

Cemadotin Binds to an Apparently Novel Site in Tubulin. Many antimitotic compounds of diverse structure bind in one of two major ligand binding domains in tubulin, known as the vinca alkaloid binding domain and the colchicine binding domain (*36*, *37*). However, in previous studies using a nonequilibrium centrifugal gel-filtration method to examine the binding of radiolabeled cemadotin to tubulin, the drug did not detectably inhibit the binding of either vinblastine or colchicine to tubulin (*6*). Cemadotin is one of the dolastatin family of antimitotic compounds. In the dolastatin family, dolastatin 10 is a noncompetitive inhibitor of vinblastine binding to tubulin and is thought to bind in the "peptide binding site", near the vinca binding site and within the vinca binding domain (*37*). In contrast, dolastatin 15 (the parent compound of cemadotin) does not detectably inhibit vinblastine binding (*10*).

Using an independent method that assays changes in tubulin fluorescence under equilibrium binding conditions, we confirmed that cemadotin does not inhibit the binding of vinblastine to tubulin. Since vinblastine binding to tubulin quenches the inherent fluorescence of tubulin (*38*), we reasoned that if cemadotin could inhibit the binding of vinblastine to tubulin, incubation of tubulin with cemadotin should eliminate the vinblastine-induced quenching of tubulin fluorescence. However, cemadotin at concentrations as high as 200 μM had no effect on the quenching of tubulin fluorescence induced by vinblastine (3−10 μM), thus confirming that cemadotin does not inhibit the binding of vinblastine to tubulin.

In the second approach, we examined the converse, that is, whether vinblastine inhibits the binding of [^{14}C]cemadotin to tubulin. Tubulin (5 μM) was incubated with 10 μM of [^{14}C]cemadotin in the absence and presence of a range of concentrations of vinblastine (10−50 μM). Vinblastine had no effect on the binding of [^{14}C]cemadotin to tubulin (data not shown). Thus we detected no competition between the binding of vinblastine and cemadotin to tubulin, suggesting that cemadotin binds to a novel site on tubulin.

Cemadotin Induced Little or No Conformational Change in Tubulin. We used several fluorescence spectroscopic assays to search for possible effects of cemadotin binding on tubulin conformation (Experimental Procedures). In the first assay, we found that cemadotin had no significant effect on the intrinsic tryptophan fluorescence of tubulin. At 200 μM, the drug quenched intrinsic tubulin fluorescence by less than 5%. Increasing the Mg^{2+} concentration (to 6 mM) also did not alter the fluorescence of tubulin upon binding by cemadotin (data not shown).

Bis-8-anilino-1-naphthalenesulfonic acid (bis-ANS) is a fluorescent ligand that is widely used to monitor conformational changes in tubulin (*39*, *40*). Incubation of tubulin with cemadotin at concentrations as high as 200 μM had no detectable effect on the tubulin−bis-ANS fluorescence (data not shown).

The apolar molecule 1-anilino-8-naphthalenesulfonate (ANS) stoichiometrically binds to tubulin at a single site, and the tubulin−ANS complex fluoresces strongly, making it a useful tool for probing conformational states of the tubulin dimer (*41*). As shown in Figure 8, the binding of vinblastine (30 μM) to tubulin increased the fluorescence of

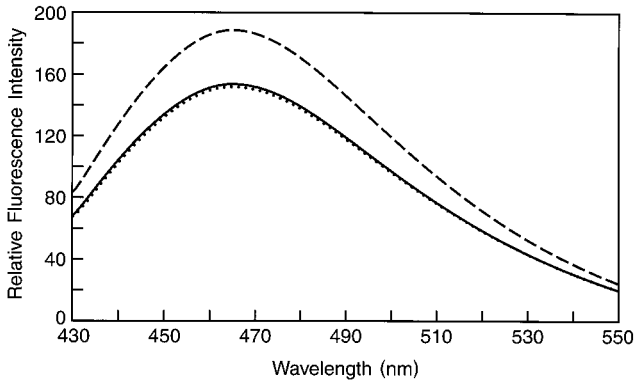

FIGURE 8: Absence of effect of cemadotin (100 μM) on the fluorescence of tubulin−ANS complex as compared with the effect of vinblastine (30 μM). Tubulin (3 μM) was incubated with cemadotin for 30 min at 34 °C. ANS (50 μM) was added and fluorescence was measured 15 min later. The excitation and emission wavelengths were 400 and 468 nm, respectively. Fluorescence in control (solid line) and in the presence of vinblastine (dashed line) or cemadotin (dotted line) is plotted.

the tubulin−ANS complex. However, cemadotin, at concentrations as high as 100 μM, had no effect on the fluorescence of the tubulin−ANS complex (Figure 8). Together these results indicate that binding of cemadotin to tubulin does not perturb the tryptophan residues of tubulin and does not detectably alter the tertiary structure of tubulin.

DISCUSSION

Cemadotin is a potent antiproliferative agent that acts by blocking cells at mitosis. Previously it was unclear whether the drug acted primarily on microtubules or whether it had another cellular target. In this study we found that cemadotin binds to tubulin. Importantly, it also strongly suppresses the dynamics of individual microtubules in vitro. Cemadotin exerts its suppressive effects on microtubule dynamics by reducing the rate and extent of both growing and shortening excursions and by increasing the time microtubules spend in the attenuation state, neither growing nor shortening detectably. Dynamic microtubules are important to mitosis in a number of ways: in the proper formation of the mitotic spindle, in the "search and capture" process of attachment of chromosomes to spindle microtubules, in chromosome congression to the metaphase equatorial plate, in the transition from metaphase to anaphase, and in anaphase movement to the spindle poles (*19*, *20*, *42*). There is strong evidence that suppression of the rates, lengths, and transition frequencies of microtubule growing and shortening events during mitosis are the most potent mechanism of action of several antimitotic drugs, including vinblastine, taxol, estramustine, and, as shown here, the dolastatin analogue cemadotin.

Interaction with Tubulin. We found that cemadotin binds to tubulin in two different classes of binding sites, a high-affinity class of sites with a dissociation constant of 19.4 μM, and a low-affinity class of sites with a dissociation constant of 136 μM. Since cemadotin induces aggregation of tubulin into small discrete rings or partial ring structures (*6*), it is possible that the low-affinity site is produced by aggregation of tubulin dimer into oligomers in the presence of cemadotin.

The binding of cemadotin to tubulin is unusual in that it produced no detectable conformational alteration in tubulin. Binding of the drug did not perturb the intrinsic tryptophan fluorescence of tubulin or the fluorescence of the tubulin−bis-ANS complex or the tubulin−ANS complex (Figure 8). The related peptide compound dolastatin 10 was found to bind in the vinca alkaloid binding domain in tubulin (*37*). However, by fluorescence quenching methods, we confirmed the results of de Arruda et al. (*6*), indicating that cemadotin does not inhibit the binding of vinblastine to tubulin. Conversely, we also found that vinblastine does not inhibit the binding of radiolabeled cemadotin to tubulin. These results indicate that cemadotin binds to a site different from the vinblastine site on tubulin. Previous studies also indicated that the compound does not bind to the colchicine site in tubulin (*6*); thus the drug may bind to a novel site in tubulin.

The interaction of cemadotin with tubulin appears to be significantly stronger than the interaction of the parent compound dolastatin 15 with tubulin. Cemadotin binds to tubulin (Figure 6) and induces tubulin aggregation (*6*), indicating that the drug increases the association of tubulin dimers. Unlike cemadotin, neither the binding of dolastatin 15 to tubulin nor the induction of tubulin aggregation has been detected. In addition, dolastatin 15 only weakly inhibits the polymerization of tubulin, with a K_i of 23 μM (*10*), as compared with a K_i of 1 μM for cemadotin (Figure 2).

Cemadotin Must Bind to Microtubule Ends. Inhibition of microtubule polymerization occurred in a concentration-dependent manner with half-maximal inhibition at 1 μM drug. At this concentration, the ratio of total tubulin to cemadotin was 18:1. Thus cemadotin is a substoichiometric inhibitor of microtubule polymerization. Substoichiometric inhibition of microtubule assembly must involve binding of the drug to the ends of the microtubules by the drug molecule acting alone or as a complex with soluble tubulin. In addition, microtubule dynamics were stabilized by cemadotin regardless of how high the final critical concentration of soluble tubulin achieved. For example, cemadotin (100 nM) inhibited microtubule polymerization by 38% and increased the concentration of soluble tubulin (from 9 to 12 μM), but the microtubules that formed were kinetically stabilized (Figure 2B), indicating that cemadotin must interact with microtubule ends.

Cemadotin Potently Suppresses Microtubule Dynamics. Cemadotin suppressed the rates and lengths of growth and shortening, increased the percentage of time that microtubules spent in a phase of attenuation or pause, and enhanced the frequency of rescue with little effect on the frequency of catastrophe (Figures 3−5, Table 1). The rate of growing was suppressed by a larger percentage than the rate of shortening. This is unusual as the antimitotic drugs examined so far either preferentially suppress the rate of shortening (taxol, colchicine, cryptophycin) or suppress the rates of shortening and growing equivalently (vinblastine, estramustine) (*25*, *26*, *28*, *32*, *43*−*45*). The mechanistic reason for this difference is not clear.

Cemadotin (10−100 nM) reduced the growing rate in the presence of a slight increase in the soluble tubulin concentration (soluble tubulin increased from ∼10 μM in the absence of drug to ∼11 μM in the presence of 100 nM drug). Thus the reduction of growing rate was not due to a decrease of assembly-competent tubulin but must be due to binding of the drug to the microtubules. We do not know whether cemadotin suppresses dynamics by interacting only at

microtubule ends like vinblastine or whether it binds to the ends and also incorporates into the polymer as does the tubulin−colchicine complex. The binding of a few molecules of cemadotin or cemadotin−tubulin complex at or near the microtubule end may induce a strain in the tubulin lattice at the microtubule end by steric hindrance. To relieve the strain, the newly added tubulin may adopt an incorrect geometry that makes future tubulin addition energetically unfavorable. As a result the growing rate will decrease. Thus the binding of cemadotin at the microtubule end may stop growth transiently and/or may induce a phase of pause or attenuation. Once the molecule of cemadotin has dissociated from the end or become buried inside the lattice, growth can resume. Cemadotin also reduced the shortening rate. To reduce the shortening rate cemadotin may bind and stabilize the end long enough so that addition of tubulin molecules can occur to the depolymerizing end of a microtubule. The binding of cemadotin may stabilize the interaction between the tubulin dimers in a manner related to its induction of tubulin aggregation, reducing the intrinsic dissociation rate of tubulin.

The frequencies of catastrophe (transition from growing or attenuated states to shortening) and rescues (transitions from shortening to growth or attenuated states) are important for the regulation of microtubule dynamics in cells. Tubulin assembles with GTP present on the β-tubulin exchangeable site. Subsequently GTP is hydrolyzed to produce GDP so that the bulk of the microtubule surface lattice is composed of tubulin-GDP. It is thought that microtubules continue to elongate as long as they maintain a cap of tubulin-GTP at their ends, and loss of the stabilizing cap from the end of the microtubule induces a catastrophe. Cemadotin did not affect the catastrophe frequency, suggesting that it does not act directly on the capping mechanism. Regain of the cap by addition of tubulin-GTP allows rescue of the depolymerizing microtubules by preventing further subunit loss and promoting regrowth. Cemadotin increased the rescue frequency, possibly by strengthening intertubulin interactions at the microtubule end and/or by reducing the shortening rate, thus allowing more time during a shortening event for cap regain.

Low concentrations of cemadotin stabilized the dynamics of microtubules without greatly changing the polymer mass. Similarly, vinblastine, colchicine, estramustine, cryptophycin, and taxol suppress microtubule dynamics at low concentrations without appreciably changing the microtubule mass (*25*, *28*, *32*, *43*, *45*). Each antimitotic drug so far characterized binds in a unique manner to tubulin or to microtubules and each drug has unique suppressive effects on microtubule dynamics. Cemadotin acts primarily by suppressing the rates of growth and shortening and enhancing the frequency of rescue with little effect on the frequency of catastrophe. At very high concentrations (micromolar) it appears to induce microtubule depolymerization by binding to soluble tubulin and preferentially inducing the formation of small oligomers or tubulin aggregates rather than microtubules. Interestingly, these actions appear to occur with no detectable alteration in the conformation of tubulin. Thus cemadotin is an unusual suppressor of microtubule dynamics with a unique molecular mechanism of action. Cemadotin appears to exert its antiproliferative effects by stabilizing spindle microtubule dynamics through a novel interaction with tubulin.

ACKNOWLEDGMENT

We gratefully acknowledge stimulating discussions with Dr. Leslie Wilson and Dr. Richard Himes. Bovine brain tubulin and flagellar axonemes were kindly prepared by Mr. Herb Miller.

REFERENCES

1. Luduena, R., Roach, M., Prasad, V., and Pettit, G. (1992) *Biochem. Pharmacol. 43*, 539−543.
2. Pettit, G. R., Kamano, Y., Fujii, Y., Inoue, M., Brown, P., Gust, D., Kitahara, K., Schmidt, J. M., Doubek, D. L., and Michel, C. J. (1981) *J. Nat. Prod. 44*, 482−485.
3. Steube, K., Grunicke, D., Pietsch, T., Gignac, S., Pettit, G., and Drexler, H. (1992) *Leukemia 6*, 1048−1053.
4. Beckwith, M., Urba, W. J., and Longo, D. L. (1993) *J. Natl. Cancer Inst. 85*, 483−488.
5. Garteiz, D. A., Madden, T., Beck, D. E., Huie, W. R., McManus, K. T., Abbruzzese, J. L., Chen, W., and Newman, R. A. (1998) *Cancer Chemother. Pharmacol. 41*, 299−306.
6. de Arruda, M., Cocchiaro, C. A., Nelson, C. M., Grinnell, C. M., Janssen, B., Haupt, A., and Barlozzari, T. (1995) *Cancer Res. 55*, 3085−3092.
7. Jordan, M. A., Thrower, D., and Wilson, L. (1991) *Cancer Res. 51*(8), 2212−22.
8. Jordan, M. A., Thrower, D., and Wilson, L. (1992) *J. Cell Sci. 102*, 401−16.
9. Jordan, M. A., Toso, R. J., Thrower, D., and Wilson, L. (1993) *Proc. Natl. Acad. Sci. U.S.A. 90*, 9552−9556.
10. Bai, R. B., Friedman, S. J., Pettit, G. R., and Hamel, E. (1992) *Biochem. Pharmacol. 43*, 2637−2645.
11. Hyams, J. S., and Lloyd, C. W. (Eds.) (1994) *Microtubules*, Wiley-Liss, Inc., New York.
12. Mitchison, T. J., and Kirschner, M. (1984) *Nature 312*, 237−242.
13. Horio, T., and Hotani, H. (1986) *Nature 321*, 605−607.
14. Walker, R. A., O'Brien, E. T., Pryer, N. K., Soboeiro, M. F., Voter, W. A., Erickson, H., and Salmon, E. D. (1988) *J. Cell Biol. 107*, 1437−1448.
15. Erickson, H. P., and O'Brien, E. T. (1992) *Annu. Rev. Biophys. Biomol. Struct. 21*, 145−166.
16. Carlier, M.-F. (1989) *Int. Rev. Cytol. 115*, 139−170.
17. McIntosh, J. R., and Hering, G. E. (1991) *Annu. Rev. Cell Biol. 7*, 403−426.
18. Wordeman, L., and Mitchison, T. J. (1994) in *Microtubules* (Hyams, J. S., Lloyd, C. W., Eds.) pp 287−302, Wiley-Liss, New York.
19. Wilson, L., and Jordan, M. A. (1995) *Chem. Biol. 2*, 569−573.
20. Jordan, M. A., and Wilson, L. (1998) *Curr. Opin. in Cell Biol. 10*, 123−130.
21. Wilson, L., and Jordan, M. A. (1994) in *Microtubules* (Hyams, J. S., and Lloyd, C., Eds.) pp 59−84, John Wiley and Sons, Inc., New York.
22. Dhamodharan, R. I., Jordan, M. A., Thrower, D., Wilson, L., and Wadsworth, P. (1995) *Mol. Biol. Cell 6*, 1215−1229.
23. Jordan, M. A., Wendell, K. L., Gardiner, S., Derry, W. B., Copp, H., and Wilson, L. (1996) *Cancer Res 56*, 816−825.
24. Jordan, M. A., and Wilson, L. (1995) in *Taxane Anticancer Agents.* (Georg, G. I., Chen, T. T., Ojima, I., Vyas, D. M., Eds.) pp 138−153, American Chemical Society, Washington, DC.
25. Derry, W., B., Wilson, L., and Jordan, M. A. (1995) *Biochemistry 34*, 2203−2211.
26. Toso, R. J., Jordan, M. A., Farrell, K. W., Matsumoto, B., and Wilson, L. (1993) *Biochemistry 32* (5), 1285−1293.
27. Bradford, M. M. (1976) *Anal. Biochem. 72*, 248−254.
28. Panda, D., Jordan, M. A., Chin, K., and Wilson, L. (1996) *J. Biol. Chem. 271*, 29807−29812.
29. Wood, D. L., Panda, D., Wiernicki, T. R., Wilson, L., Jordan, M. A., and Singh, J. P. (1997) *Mol. Pharmacol. 52*, 437−444.

30. Singer, W. D., Hersh, R. T., and Himes, R. H. (1988) *Biochem. Pharmacol. 37*, 2691−2696.
31. Scatchard, G. (1949) *Ann. N.Y. Acad. Sci. 51*, 660−692.
32. Panda, D., Miller, H., Islam, K., and Wilson, L. (1997) *Proc. Natl. Acad. Sci. U.S.A. 94*, 10560−10564.
33. Belmont, L., Hyman, A. A., Sawin, K. E., and Mitchison, T. J. (1990) *Cell 62*, 579−589.
34. Gliksman, N. R., Skibbens, R. V., and Salmon, E. D. (1993) *Mol. Biol. Cell 4*, 1035−1050.
35. Kowalski, R. J., and Williams, R. C., Jr. (1993) *J. Biol. Chem. 268*, 9847−9855.
36. Bai, R. B., Pettit, G. R., and Hamel, E. (1990) *Biochem. Pharmacol. 39*, 1941−1949.
37. Bai, R. B., Pettit, G. R., and Hamel, E. (1990) *J. Biol. Chem. 265*, 17141−17149.
38. Lee, J. C., Harrison, D., and Timasheff, S. N. (1975) *J. Biol. Chem. 250*, 9276−9282.
39. Panda, D., Singh, J. P., and Wilson, L. (1997) *J. Biol. Chem. 272*, 7681−7687.
40. Prasad, A. R. S., Luduena, R. F., and Horowitz, P. M. (1986) *Biochemistry 25*, 739−742.
41. Battacharyya, B., and Wolff, J. (1975) *Arch. Biochem. Biophys. 167*, 264−269.
42. Rieder, C. L., Cole, R. W., Khodjakov, A., and Sluder, G. (1995) *J. Cell Biol. 130*, 941−948.
43. Panda, D., Daijo, J. E., Jordan, M. A., and Wilson, L. (1995) *Biochemistry 34*, 9921−9929.
44. Panda, D., Himes, R. H., Moore, R. E., Wilson, L., and Jordan, M. A. (1997) *Biochemistry 42*, 12948−12953.
45. Panda, D., DeLuca, K., Williams, D., Jordan M. A., and Wilson, L. (1998) *Proc. Natl. Acad. Sci. U.S.A. 95*, 9313−9318.

BI9817414